

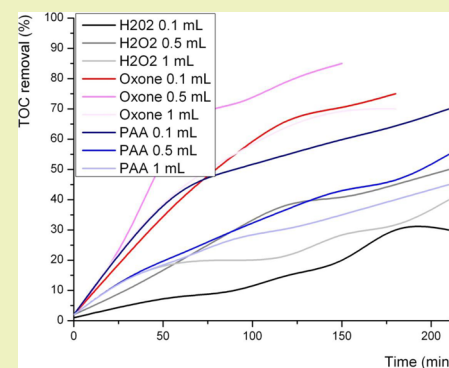
Eco-Friendly Magnetic Iron Oxide-Pillared Montmorillonite for Advanced Catalytic Degradation of Dichlorophenol

Jurate Virkutyte^{†,*} and Rajender S. Varma^{‡,*}[†]Hammontree and Associates, Ltd., 4364 Whitmore Lane, Fairfield, Ohio 45014, United States[‡]Sustainable Technology Division, National Risk Management Research Laboratory, U.S. Environmental Protection Agency, 26 West M. L. K. Drive, MS 443, Cincinnati, Ohio 45268 United States

Supporting Information

ABSTRACT: Eco-friendly pillared montmorillonites, in which the pillars consist of iron oxide, are expected to have interesting and unusual magnetic properties that are applicable for environmental decontamination. A completely “green” and effective composite was synthesized using mild reaction conditions and benign products. The composite was characterized by scanning electron microscopy (SEM) equipped with EDS, transmission electron microscopy (TEM), X-ray diffraction (XRD), and thermogravimetric analysis (TGA). Catalytic activity was tested against the degradation of dichlorophenol (DCP) and was found that in the presence of peroxymonosulfate 85% of DCP disappeared in 2.5 h, whereas in the presence on hydrogen peroxide and peracetic acid nearly 50% and 70% of DCP, respectively, degraded in 3.5 h. TOC showed about 85% demineralization of the solution, which indicates a successful degradation of DCP.

KEYWORDS: γ - Fe_2O_3 , Montmorillonite, Nanocomposite, Dichlorophenol, Degradation, TOC



INTRODUCTION

Environmental contamination with various organic compounds is currently one of the most urgent problems that the scientific community as well as general public has to face; therefore, various methods for organic decontamination have been extensively studied over the last few decades. These methods and approaches include electrochemical techniques, advanced oxidation, adsorption on porous surfaces, and biodegradation to name a few.¹ To date, considerable attention has been directed to the degradation of organic compounds via adsorption and advanced catalytic oxidation (ACO) in the presence of various oxidants. The principles of ACO are based on the *in situ* generation of reactive oxygen species such as hydroxyl radicals, superoxide anions, sulfate radicals, etc. for the oxidation of organic compounds that may lead to complete mineralization.² Despite a great number of available ACO processes (e.g., O_3 , H_2O_2 , ultraviolet (UV), and microwave and ultrasound (US) irradiation, as well as their combinations thereof), there is still a continuous search for more effective strategies to generate radicals to destroy organic contaminants.³

Smectite clays are a class of layered aluminosilicates that exhibit unique swelling, intercalation, and ion-exchange properties that make them excellent materials for various industrial applications including environmental restoration and remediation as adsorbents and fillers.⁴ Clays loaded or intercalated with various metals and/or metal oxides constitute a new class of composites.⁵ Iron is a benign and extremely important earth-abundant element in the environment because of its presence in the chemistry of soils and natural waters under the form of

molecular complexes and/or colloids.⁶ Also, Fe-based minerals and Fe ions are effectively utilized for heterogeneous and homogeneous Fenton processes that are one of the most popular and effective organic contaminant degradation processes.⁷ Therefore, the combination of iron/iron oxides and clays may offer numerous advantages over conventionally accepted Fenton and Fenton-like processes.

Clays modified with magnetic iron oxides are regarded as very promising materials for environmental applications.⁸ Herein, we present a simple and facile synthesis of Fe_2O_3 -montmorillonite using benign reaction precursors and mild reaction conditions. The as-prepared composite was characterized in detail with XRD, SEM, TEM, and TGA. Its catalytic activity was tested against the degradation of DCP in the solution, and its stability was examined in 5 consecutive runs. Total mineralization of the solution was also assessed in terms of the TOC.

EXPERIMENTAL SECTION

Chemicals. All the chemicals were used as received without further purification. Montmorillonite K10 (main chemical composition of SiO_2 (69%), Al_2O_3 (14.6%), Fe_2O_3 (2.9%), MgO (2%), and CaO (1.5%), cation exchange capacity (CEC) of 110 meq/100 g^{-1} , and surface area of 220–270 $\text{m}^2 \text{g}^{-1}$), dichlorophenol (DCP), FeCl_3 , and

Special Issue: Sustainable Nanotechnology 2013

Received: February 16, 2014

Published: April 23, 2014

$\text{FeCl}_2 \cdot 4\text{H}_2\text{O}$ were obtained from Sigma-Aldrich (U.S.A.). Double distilled water was used in all the experiments.

Synthesis of $\gamma\text{-Fe}_2\text{O}_3$. For the synthesis of monodisperse $\gamma\text{-Fe}_2\text{O}_3$ nanoparticles, 16.2 g (20 mmol) of FeCl_3 and 9.9 g (10 mmol) of $\text{FeCl}_2 \cdot 4\text{H}_2\text{O}$ along with 10 g of urea were dissolved in 500.0 mL of distilled water. The mixture was continuously stirred for 60 min at 90 °C in a water bath before cooling to room temperature (22 ± 1 °C). The precipitates were centrifuged at 4500 rpm and washed first with deionized water then with ethanol. Subsequently, precipitates were dried at 75 °C overnight, and the collected powders were calcined at 600 °C in air. The resultant $\gamma\text{-Fe}_2\text{O}_3$ was used to prepare the Fe_2O_3 -montmorillonite composite.

During a typical synthesis, montmorillonite K10 (10 g), dried at 80 °C overnight to remove accumulated moisture, was slurred with 15 g of $\gamma\text{-Fe}_2\text{O}_3$ (dissolved in 60 mL of deionized water). The ensuing slurry was sonicated for 30 min and magnetically stirred at room temperature for 3 h. Then Fe_2O_3 -montmorillonite was filtered, five times washed with deionized water, and dried in air at 60 °C for 12 h. After drying, samples were crushed to a fine powder and subsequently activated at 400 °C for a period of 2 h with 5 °C min^{-1} in air.⁹ The composite was stored in closed vials and used when required after overnight activation at 120 °C to remove accumulated moisture.

Characterization of the Nanocomposites. The X-ray diffraction (XRD) patterns of as-prepared nanocomposites and commercially available Degussa P25 (for comparison) were recorded on a X'Pert Pro MPD X-ray diffractometer with a $\text{Cu K}\alpha$ source and diffraction angle range of $2\theta = 10\text{--}80^\circ$ with a count time of 20 s at each point. The accelerating voltage and applied current were 45 kV and 40 mA, respectively. The average crystallite size (D_p) was calculated as a function of the peak width according to the Scherrer's equation

$$D_p = \frac{0.9\lambda}{\beta \cos \theta} \quad (1)$$

where D_p is the crystallite size (nm), λ is X-ray wavelength (0.154056 nm), θ is the Bragg angle, and β is full width at half-maximum (fwhm). fwhm of each diffraction line was determined from the profile measured with a scanning rate of $1/2^\circ$ (2θ) min^{-1} , which was calibrated by standard silicon powder for instrumental broadening. The phases were identified by using Joint Committee on Powder Diffraction Standards (JCPDS).

The morphology of samples was evaluated using scanning electron microscopy (FEI XL 30 ESEM) equipped with EDS (energy dispersive X-ray spectroscopy) operating at 15–20 kV on gold-sputtered samples. High-resolution transmission electron microscopic (HR-TEM) images were recorded using a FEI CM20 TEM operating at an accelerated voltage of 60–120 keV.

Thermogravimetric analysis (TGA) was performed using a TGA Q5000 (TA Instruments) analyzer with a heating rate of 5 degrees/min in air adopting a ramp method (temperature increase from 100 to 800 °C).

Degradation Experiments. After the preliminary experiments (data not shown), the rate of DCP (Figure SI 1, Supporting Information) degradation was found to obey pseudo-first-order reaction kinetics, and therefore, the photodegradation rate constant, k (min^{-1}) was obtained according to the power rate law

$$C = C_0 e^{-kt} \quad (2)$$

where C is the DCP concentration (mg L^{-1}), t is time (min), and k is the pseudo-first-order reaction rate constant (min^{-1}).

DCP solutions (100 mg L^{-1}) were prepared by dissolving the appropriate amounts of the contaminants in deionized water to reach the required initial concentration. The batch adsorption experiments were carried out in 100 mL closed glass containers where 0.05 g of the catalyst (concentration of 1 g L^{-1}) and 50 mL of the target contaminant was added. The typical catalytic activity was tested at room temperature (25 ± 1 °C) in a 100 mL glass flask. Changes in TOC were monitored on a Shimadzu TOC V CPH for non-purgeable organic carbon.

RESULTS AND DISCUSSION

Characterization. The preparation of magnetic iron oxide-loaded and/or -exchanged montmorillonite was performed utilizing the green synthesis route without the addition of hazardous chemicals and using mild reaction conditions. It was hypothesized that interlayer sodium cations were exchanged for iron(III) cations. Figure 1 shows the XRD pattern of Fe_2O_3 -

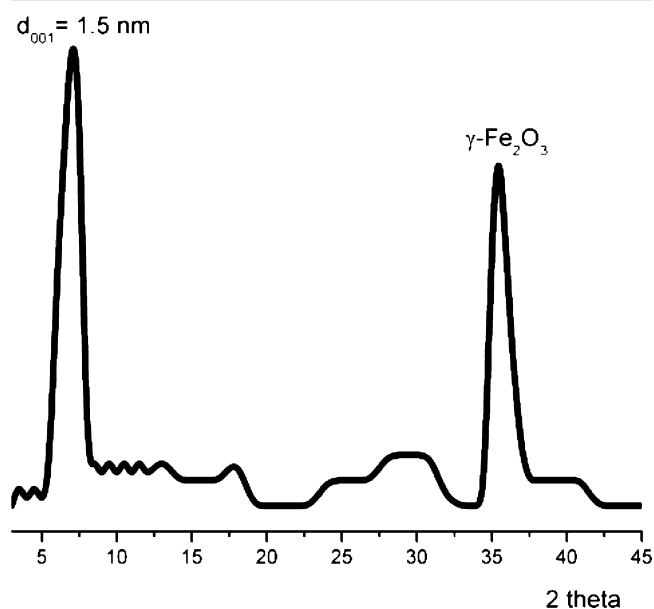


Figure 1. XRD patterns of $\gamma\text{-Fe}_2\text{O}_3$ -montmorillonite.

montmorillonite. Evidently, the loading of montmorillonite with $\gamma\text{-Fe}_2\text{O}_3$ changed the d_{001} parameter of the parent montmorillonite from 12.5 Å to about 15 Å. This is consistent with findings of Bourlinos and colleagues⁴ who researched the synthesis and characterization of magnetically modified clays and found that magnetic iron particles significantly increase the d_{001} indicating the successful replacement of sodium ions with those of iron. In addition, the peak at 35.7° indicated the formation of $\gamma\text{-Fe}_2\text{O}_3$ with the dimensions of about 102 Å as determined by the Scherrer equation. It was hypothesized that iron oxide particles were dispersed on the external surfaces of montmorillonite with protons, fixed during the synthesis procedure, and also acted as balancing cations.

Figure 2 shows the micrographs of morphologies of Fe_2O_3 -montmorillonite studied by SEM and TEM. The atomic surface composition (%) and EDX data are given as insets. A general view of the composite is shown in Figure 2a (TEM) and b (SEM). Evidently, the composite had near spherical aggregated particles with particles about 10–15 nm (Figure 2a). As shown in Figure 2b, a typical sheet-like structure can be evidenced in the low magnification micrograph, which is generally accepted for clay-type materials.¹⁰ However, the inset in Figure 2b showing a high magnification micrograph indicated the formation of material with two different textures that is the rather flat surface of a clay and iron oxide aggregate. Elemental surface composition showed the occurrence of O K (64%), Al K (0.15%), Si K (0.53%), and S K (1.39%), which might be attributed to the parental montmorillonite surface composition, whereas Cl K (14.42%) could be assigned to the reaction precursors and Fe K (18.77%) to the magnetic iron oxide on the surface of the clay. Furthermore, EDAX data strongly

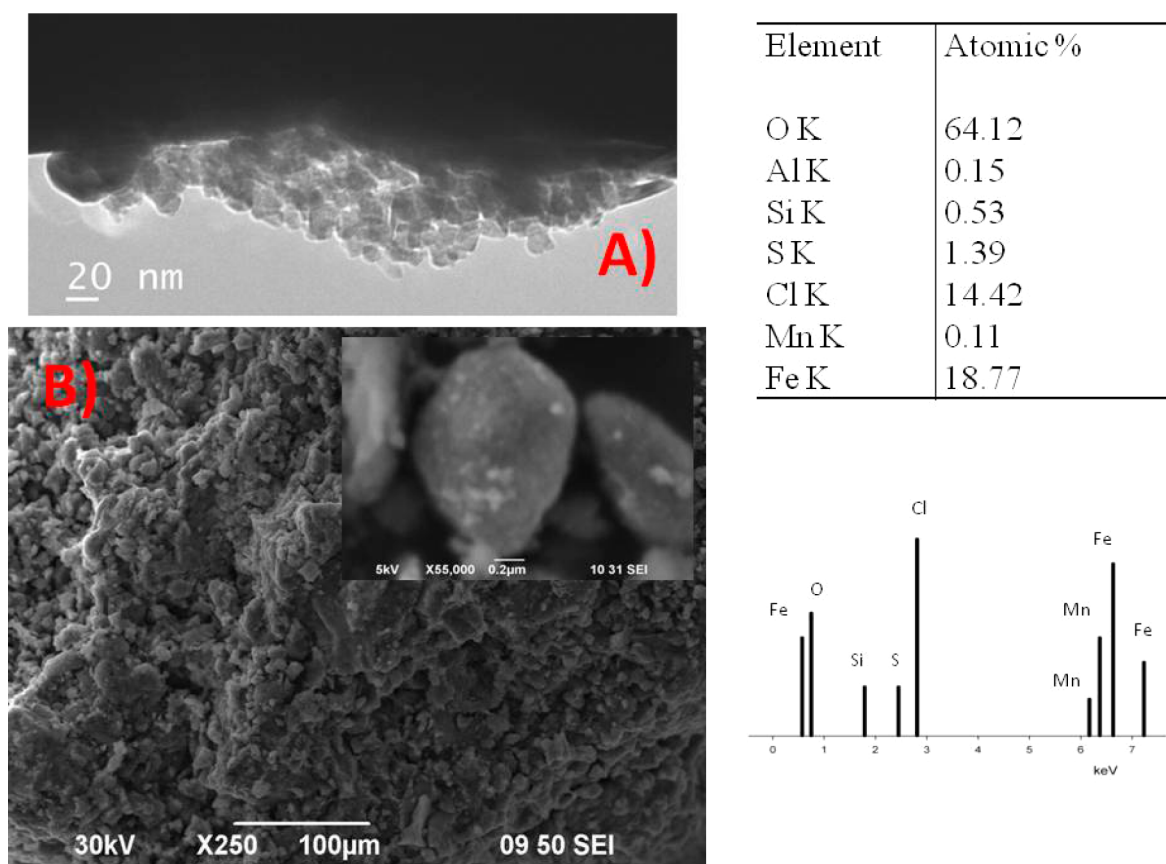


Figure 2. (a) TEM and (b) SEM (high-resolution image as inset) micrographs of γ - Fe_2O_3 -montmorillonite along with surface % composition and EDAX data.

suggested that Fe was incorporated onto the surface of the montmorillonite.

Thermogravimetric analysis graphs of montmorillonite K10 and Fe_2O_3 -montmorillonite are given in Figure 3.

Nearly 5% and 11% of weight loss up to 250 °C in montmorillonite and Fe_2O_3 -montmorillonite could be attributed to the loss of adsorbed water and some of the reaction

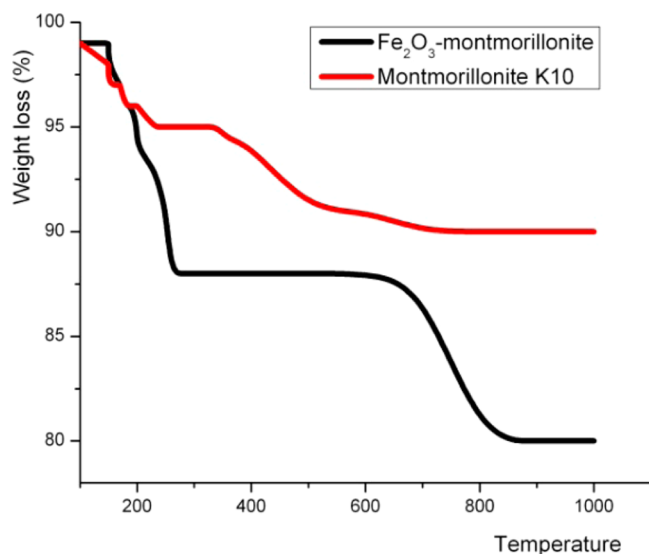


Figure 3. Thermogravimetric analysis of γ - Fe_2O_3 -montmorillonite and parent compound montmorillonite K10.

precursors.¹¹ Additionally, less than 10% weight loss for Fe_2O_3 -montmorillonite and about 4% for montmorillonite was observed in the range between 400 to 750 °C, which could be attributed to the dehydroxylation of hydroxide groups associated with interlayer pillars of clay and/or structural water still present in the layers of montmorillonite.^{11,12}

Degradation of Dichlorophenol (DCP) in the Presence of Oxidants and Fe_2O_3 -Montmorillonite. The catalytic activity of Fe_2O_3 -montmorillonite for the degradation of DCP was evaluated in the presence of hydrogen peroxide (30% vol), oxone (0.1 M), and peracetic acid (15% vol). Before the actual degradation experiments, DCP was subjected to the sorption onto the composite to establish the baseline for the catalytic degradation experiments in the presence of the oxidants. The adsorption was performed in the dark, and it was established that about 25% of DCP was adsorbed onto the surface of a composite (data not shown). However, the overall adsorption onto the surface of the composite was rather limited; thus, only catalytic degradation of DCP was taken into account and included into the discussions.

According to Feng and colleagues,¹³ degradation of organic compounds follows two distinct pathways: (1) catalytic activity from Fe_2O_3 -montmorillonite, which is activated by the oxidants and possibly (2) Fe ions that are leached out from the surface of the montmorillonite. However, when the pH was significantly reduced, no iron deposition was observed suggesting that the main contribution toward degradation of DCP is from the Fe_2O_3 -montmorillonite catalyst.

It is widely accepted that the concentration or the amount of the oxidant plays an important role in the degradation of

organic contaminants. According to Dhananjeyan and colleagues,¹⁴ concentration of the oxidants, for instance, H₂O₂ is directly related to the number of *OH radicals generated during the reaction. Thus, the degradation rate increases as the oxidant concentration increases until a critical concentration of an oxidant is reached. When the concentration of an oxidant is higher than a critical concentration, the degradation rates of organic contaminants will decrease due to the self-scavenging effect.

Hydrogen Peroxide. Degradation of DCP in the presence of 0.1, 0.5, and 1 mL of hydrogen peroxide in 100 mL of the solution in the presence of 1 g L⁻¹ composite was carried up to 210 min. Details can be found in Figure SI 2 of the Supporting Information. Degradation of DCP was the lowest when 0.1 mL of H₂O₂ concentration was used and the highest when 0.5 mL of an oxidant was used. Furthermore, when the concentration was increased to 1 mL, degradation of DCP was retarded, suggesting that the critical concentration was reached and the self-scavenging effect occurred.¹⁵

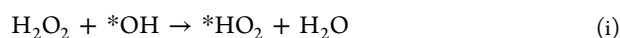


Figure 4 showed that the use of hydrogen peroxide did not significantly increase the reaction rates of DCP degradation

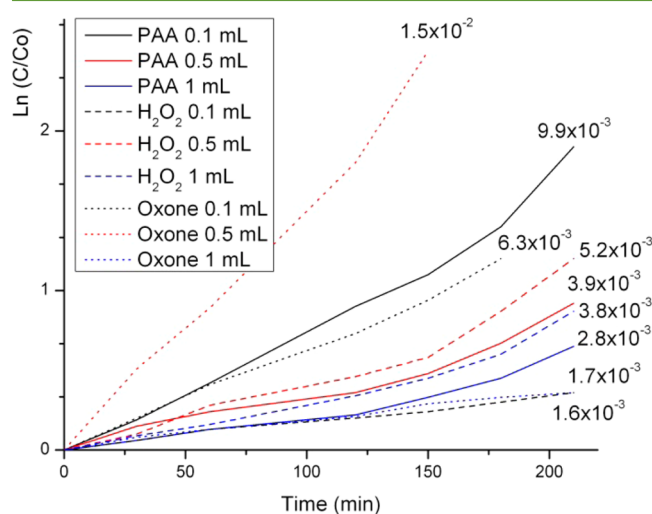
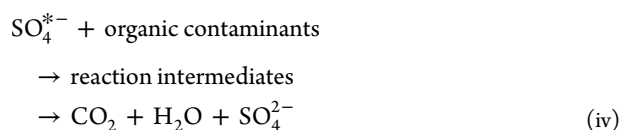
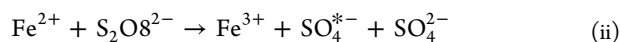


Figure 4. Disappearance of DCP in the presence of various concentrations of hydrogen peroxide, oxone, and peracetic acid with reaction constants.

(H₂O₂ 0.5 mL, 5.2 × 10⁻³ min⁻¹), suggesting that the nanocomposite was not effective in activating the oxidant.

Oxone. The formation of sulfate radicals (SO₄^{*-}) and its interaction with organic contaminants is as follows¹⁶



Furthermore, degradation of DCP in the presence of oxone was probably due to (i) the rapid sulfate radical generation that reacted with DCP and (ii) potential recombination of lower sulfate radicals in the solution, production of weaker

peroxysulfate radicals by Fe₂O₃-montmorillonite, and slow reactivation of the nanocomposite.¹⁷ The latter may have hindered the overall DCP degradation efficiency.

Figure 4 presents the degradation and reaction rates of DCP in the presence of various amounts of oxone. Evidently, the highest reaction rates were obtained when 0.5 mL of oxone was introduced (1.5 × 10⁻² min⁻¹), followed by 0.1 mL (6.3 × 10⁻³ min⁻¹). Unfortunately, the use of 1 mL of oxone did not result in an increased degradation as well as the reaction rates (1.7 × 10⁻³ min⁻¹), implying that an overdose or a critical concentration of the oxidant has been reached and radicals were self-scavenged, thus impairing the degradation efficiency.¹⁸ Another reason for that may be the competitive reaction for the radicals between the parent compound and the reaction intermediates.^{16,19} However, it is likely that self-scavenging of radicals took place due to all of the oxidants (hydrogen peroxide and peracetic acid) included behaving similarly to oxone. Furthermore, a significantly increased amount of the oxidant did not result in higher reaction rates or higher degradation efficiency.

Peracetic Acid. Peracetic acid is one of the most effective disinfectant agents that can also be utilized as an oxidant to destroy organic contaminants in the presence of Fe₂O₃-montmorillonite. The radical formation mechanism includes (i) the homolysis of PAA peroxy bond into two primary radicals, acyloxy (CH₃C(=O)O*) and hydroxyl (*OH),³ that can attack DCP, (ii) the acyloxy radical dissociates to a methyl radical (*CH₃) and carbon dioxide and/or a methyl radical reacts with oxygen to produce a weak peroxy (*CH₃OO) radical,²⁰ and (iii) the hydroxyl radical may react with an acyloxy radical to produce a new PAA molecule and restart the oxidation cycle.

As shown in Figure 4, the best degradation and fastest reaction rates were achieved with 1 mL of PAA (9.9 × 10⁻³ min⁻¹), followed by 0.5 mL (3.9 × 10⁻³ min⁻¹), and finally by 0.1 mL (2.8 × 10⁻³ min⁻¹), indicating that in the case of PAA, 1 mL was not an excessive amount of the oxidant and the self-scavenging effect did not take place as in comparison to hydrogen peroxide and oxone. As indicated by Rokhina and colleagues,³ the primary degradation mechanism of phenol-type contaminants over a catalyst occurs via the abstraction of an H atom from phenol followed by the formation of the radical (C₆H₅O*).

Mineralization of the Reaction Solution. During the degradation reaction, various reaction intermediates may be formed, which may be long-lived and more toxic than the parental contaminant. Thus, it is important to take mineralization into account when the main aim of the study is to research the degradation of any organic contaminants. To calculate the TOC removal (%), the following equation was used

$$\text{TOC removal (\%)} = (1 - \text{TOC}_f/\text{TOC}_i) \times 100\% \quad (3)$$

where TOC_f and TOC_i were the TOC values at the end and beginning of the reaction. Figure SI 5 of the Supporting Information presents the TOC removal of the reaction as a function of time in the presence of different amounts of oxidants. When no oxidant but the 1 g L⁻¹ composite was used, mineralization of the solution was about 8% after 210 min. This suggests that adsorption of DCP onto the surface of the composite contributed to the mineralization to some extent (data not shown). Unfortunately, the presence of Fe₂O₃-montmorillonite cannot effectively mineralize DCP, and therefore, oxidants must be employed. Mineralization signifi-

cantly increased when oxone was used as an oxidant (up to 85%) regardless of the amount used, in comparison to 30 to 70% when hydrogen peroxide and peracetic acid were employed as the oxidation agents (Figure SI 5, Supporting Information). Similar results were obtained by Rastogi and co-workers,²¹ who researched the use of a sulfate radical-based ferrous-peroxymonosulfate oxidative system to degrade persistent organic contaminants and found that the use of oxone resulted in about 80% of TOC reduction.

Importantly, the effectiveness of the oxidants (regardless of their concentration) was in the order oxone > peracetic acid > hydrogen peroxide. This may be because oxone has a higher potential than that of hydrogen peroxide and/or peracetic acid ($E^0_{\text{oxone}} = +1.82$ V, $E^0_{\text{hydrogen peroxide}} = +1.77$ V, and $E^0_{\text{peracetic acid}} = 1.81$ V).¹⁹ As aliphatics such as carboxylic acids formed by the degradation of DCP are more resistant toward further mineralization,²² a more powerful oxidant would be necessary to continue the degradation process. Thus, higher potential translated to higher mineralization of the solution.

Stability of Fe₂O₃-Montmorillonite Catalyst. A stable and effective catalyst is the key for efficient degradation of target organic contaminants; therefore, it is vital to assess the stability of the as-prepared catalyst. As pointed out by Feng and co-workers,¹³ if the stability is poor or deactivation of the catalyst is severe, then the catalyst will not be effectively utilized for various industrial applications. Five consecutive runs were performed with the same catalyst (0.5 mL of oxone) and subsequent addition of DCP to evaluate catalytic stability of composite. It was found that no actual deactivation of the catalyst was observed when compared to the first cycle using a fresh catalyst, which indicates the excellent stability in the long term and after several uses (Figure SI 6, Supporting Information). Such excellent stability could be attributed to the stable structure of Fe₂O₃-montmorillonite as confirmed by XRD measurement, where no chemical and structural changes were observed during the catalytic reaction (Figure SI 7, Supporting Information). These findings are in line with those reported for the degradation of azo dye by a photoassisted Fenton reaction utilizing an iron oxide and silicate nanocomposites.¹³ Also, compared with Fe³⁺ and Fe₂O₃-supported catalysts,^{23–25} the nanocomposite used in the current study exhibited excellent stability, efficiency, and very low production costs in comparison to other nanocomposites.

In brief, a greener synthesis protocol, employing mild reaction conditions and benign precursors, was developed for the preparation of a stable (up to five consecutive runs) and effective clay-based iron oxide nanocomposite that activated hydrogen peroxide, oxone, and peracetic acid. Furthermore, the highest DCP removal efficiency was achieved with 0.5 mL of oxone ($1.5 \times 10^{-3} \text{ min}^{-1}$), followed by 1 mL of PAA ($9.9 \times 10^{-3} \text{ min}^{-1}$), and 0.1 mL oxone ($6.3 \times 10^{-3} \text{ min}^{-1}$); their effectiveness to mineralize the solution being in the order oxone > peracetic acid > hydrogen peroxide.

It is of great importance to find innovative and simple methods and approaches to tackle environmental problems. The application of magnetic particles to solve environmental contamination is one of the most promising methods that has received increased attention from both academia and industry in recent years. Magnetic particles, especially if they are loaded onto or incorporated into cheap natural materials, such as clays, are able to adsorb contaminants from aqueous effluents without high costs and complex technical requirements. Consequently, the design and production of catalytic adsorbents with magnetic

properties is becoming very attractive and is beginning to find applications in various contaminated sites throughout the United States and globally.

■ ASSOCIATED CONTENT

Supporting Information

Chemical structure of dichlorophenol and its concentration-dependent degradation over time using hydrogen peroxide, oxone and peracetic acid and the recyclability details for the catalyst, and γ -Fe₂O₃-montmorillonite, after several cycles. This material is available free of charge via the Internet at <http://pubs.acs.org>.

■ AUTHOR INFORMATION

Corresponding Authors

*E-mail: jvirkutyte@hammontree-engineers.com (J.V.).

*E-mail: Varma.Rajender@epa.gov (R.S.V.).

Notes

The authors declare no competing financial interest.

■ ACKNOWLEDGMENTS

This research was funded and conducted by the National Risk Management Research Laboratory of U.S. Environmental Protection Agency (EPA), Cincinnati, OH. This paper has not been subjected to internal policy review of the U.S. EPA. Therefore, the research results do not necessarily reflect the views of the agency or its policy. Mention of trade names and commercial products does not constitute endorsement or recommendation for use.

■ REFERENCES

- (1) Wang, Y.-q.; Gu, B.; Xu, W.-l. Electro-catalytic degradation of phenol on several metal-oxide anodes. *J. Hazard. Mater.* **2009**, *162* (2–3), 1159–1164.
- (2) Chong, M. N.; Jin, B.; Chow, C. W. K.; Saint, C. Recent developments in photocatalytic water treatment technology: A review. *Water. Res.* **2010**, *44* (10), 2997–3027.
- (3) Rokhina, E. V.; Makarova, K.; Golovina, E. A.; Van As, H.; Virkutyte, J. Free radical reaction pathway, thermochemistry of peracetic acid homolysis, and its application for phenol degradation: Spectroscopic study and quantum chemistry calculations. *Environ. Sci. Technol.* **2010**, *44* (17), 6815–6821.
- (4) Bourlinos, A. B.; Karakassides, M. A.; Simopoulos, A.; Petridis, D. Synthesis and characterization of magnetically modified clay composites. *Chem. Mater.* **2000**, *12* (9), 2640–2645.
- (5) Skoutelas, A. P.; Karakassides, M. A.; Petridis, D. Magnetically modified Al₂O₃ pillared clays. *Chem. Mater.* **1999**, *11* (10), 2754–2759.
- (6) Jolivet, J.-P.; Chaneac, C.; Tronc, E. Iron oxide chemistry. From molecular clusters to extended solid networks. *Chem. Commun.* **2004**, *5*, 477–483.
- (7) Yap, C. L.; Gan, S.; Ng, H. K. Fenton based remediation of polycyclic aromatic hydrocarbons-contaminated soils. *Chemosphere* **2011**, *83* (11), 1414–1430.
- (8) Navratil, J. D. *Natural Microporous Materials in Environmental Technology*; Kluwer Academic Publishers: Dordrecht, 1999; Vol. 362.
- (9) Singh, D. U.; Samant, S. D. Comparative study of benzylation of benzene using benzyl chloride in the presence of pillared bentonite; ion-exchanged and pillaring solution impregnated montmorillonite K10. *J. Mol. Catal. A* **2004**, *223* (1–2), 111–116.
- (10) Oliveira, L. C. A.; Rios, R. V. R. A.; Fabris, J. D.; Sapag, K.; Garg, V. K.; Lago, R. M. Clay-iron oxide magnetic composites for the adsorption of contaminants in water. *Appl. Clay Sci.* **2003**, *22* (4), 169–177.

- (11) Virkutyte, J.; Varma, R. S. Novel claycubic to eliminate micropollutants and *Vibrio fischeri* from water. *RSC Adv.* **2012**, *2* (8), 3416–3422.
- (12) Tiwari, R. R.; Khilar, K. C.; Natarajan, U. Synthesis and characterization of novel organo-montmorillonites. *Appl. Clay Sci.* **2008**, *38* (3–4), 203–208.
- (13) Feng, J.; Hu, X.; Yue, P. L.; Zhu, H. Y.; Lu, G. Q. Degradation of azo-dye orange II by a photoassisted fenton reaction using a novel composite of iron oxide and silicate nanoparticles as a catalyst. *Ind. Eng. Chem. Res.* **2003**, *42* (10), 2058–2066.
- (14) Dhananjeyan, M. R.; Mielczarski, E.; Thampi, K. R.; Buffat, P.; Bensimon, M.; Kulik, A.; Mielczarski, J.; Kiwi, J. Photodynamics and surface characterization of TiO₂ and Fe₂O₃ photocatalysts immobilized on modified polyethylene films. *J. Phys. Chem. B* **2001**, *105* (48), 12046–12055.
- (15) Edwards, J.; Curci, R. *Catalytic Oxidation with H₂O₂ as Oxidant*; Kluwer: Dordrecht, The Netherlands, 1982.
- (16) Wang, Y. R.; Chu, W. Degradation of a xanthene dye by Fe(II)-mediated activation of oxone process. *J. Hazard. Mater.* **2011**, *186* (2–3), 1455–1461.
- (17) Wang, Y. R.; Chu, W. Degradation of 2,4,5-trichlorophenoxyacetic acid by a novel electro-Fe(II)/oxone process using iron sheet as the sacrificial anode. *Water. Res.* **2011**, *45* (13), 3883–3889.
- (18) von der Kammer, F.; Ottofuelling, S.; Hofmann, T. Assessment of the physico-chemical behavior of titanium dioxide nanoparticles in aquatic environments using multi-dimensional parameter testing. *Environ. Pollut.* **2010**, *158* (12), 3472–3481.
- (19) Wang, Y. R.; Chu, W. Photo-assisted degradation of 2,4,5-trichlorophenoxyacetic acid by Fe(II)-catalyzed activation of oxone process: The role of UV irradiation, reaction mechanism and mineralization. *Appl. B - Environ.* **2012**, *123–124* (0), 151–161.
- (20) El-Agamey, A.; McGarvey, D. J. Evidence for a lack of reactivity of carotenoid addition radicals towards oxygen: A laser flash photolysis study of the reactions of carotenoids with acylperoxyl radicals in polar and non-polar solvents. *J. Am. Chem. Soc.* **2003**, *125* (11), 3330–3340.
- (21) Rastogi, A.; Al-Abed, S. R.; Dionysiou, D. D. Sulfate radical-based ferrous–peroxymonosulfate oxidative system for PCBs degradation in aqueous and sediment systems. *Appl. Catal., B* **2009**, *85* (3–4), 171–179.
- (22) Oturan, M. A.; Peiroten, J.; Chartrin, P.; Acher, A. J. Complete destruction of p-nitrophenol in aqueous medium by electro-Fenton method. *Environ. Sci. Technol.* **2000**, *34* (16), 3474–3479.
- (23) Chen, F.; Li, Y.; Cai, W.; Zhang, J. Preparation and sono-Fenton performance of 4A-zeolite supported α -Fe₂O₃. *J. Hazard. Mater.* **2010**, *177* (1–3), 743–749.
- (24) Li, Y.; Lu, Y.; Zhu, X. Photo-Fenton discoloration of the azo dye X-3B over pillared bentonites containing iron. *J. Hazard. Mater.* **2006**, *132* (2–3), 196–201.
- (25) Liu, X.; Tang, R.; He, Q.; Liao, X.; Shi, B. Fe(III)-loaded collagen fiber as a heterogeneous catalyst for the photo-assisted decomposition of Malachite Green. *J. Hazard. Mater.* **2010**, *174* (1–3), 687–693.